Acta Physica Academiae Scientiarum Hungaricae, 53 (1—2), pp. 143—157 (1982)

FAST COMPONENTS OF THE ELECTRIC RESPONSE SIGNAL OF BACTERIORHODOPSIN PROTEIN*

L. KESZTHELYI, P. ORMOS and G. VÁRÓ

INSTITUTE OF BIOPHYSICS, BIOLOGICAL RESEARCH CENTER, SZEGED, HUNGARY

Fast electric signals corresponding to bR→K, K→L and L→M transitions in the bacteriorhodopsin photocycle were measured in cases of oriented purple membranes in solution and dried samples. In the latter case the effect of external electric field was to increase (positive field) or decrease (negative field) the transition lifetimes. Based on the existing data in visible, UV, Raman spectroscopy and electric signal a model of the bacteriorhodopsin proton pump was constructed.

1. Introduction

Bacteriorhodopsin (bR) is an integral membrane protein in the plasma mebrane of *Halobacterium halobium.* Its function is to absorb light and to convey this light energy into membrane potential and a pH gradient by pumping protons from inside the cell to its exterior [1]. These membrane gradients are then consumed by various bacterial energy requiring systems such as the ATP-ase enzymes located in the plasma membrane which synthesise ATP molecules. The so-called chemiosmotic process [2] involves essentially the same phenomena in mitochondria and chloroplasts where food energy and light energy are transformed by proton pumps into membrane potentials and pH gradients. Because proton pumps are so critical in bioenergetic processes, an understanding of their molecular mechanism is very important. The simplest systems to study are the light driven bR molecules.

The bR protein has a retinal chromophore bound to a lysine side chain (either at lysine 216 or 41) which absorbs at 570 nm and undergoes a photocycle: new absorption bands appear with different lifetimes (Fig. 1). During the cycle, protons are released at the external surface and other protons are picked up on the internal side of the plasma membrane in which bR is embedded. The bR molecules are localized in approximately 500 nm diameter discs in the so called purple membranes (pm). These pm-s can be separated from the bacteria.

The kinetic characteristics of proton movement have been studied by many authors on not well defined systems [3, 4]. A new method has been developed in our laboratory for the study of proton movement [5, 6, 7]. We have demonstrated [5] that pm-s in suspension can be oriented by low electric fields (10—15 V/cm), and that after a laser flash, protons move parallel to the field and induce measurable electrical signals in an external circuit (protein electric response signal — PERS). From the analysis of the

* Dedicated to Prof. I. Tarján on his 70th birthday.

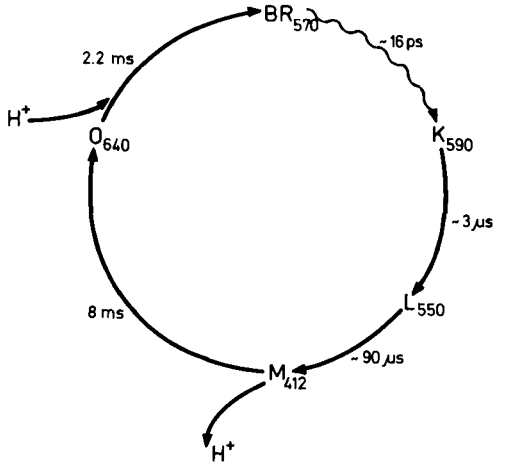

Fig. 1. The photocycle of bR. The first very fast transition to the *K*-state is light driven, the remaining ones are the consequences of thermal agitation

time course of the PERS, it has been unambiguously stated that these proton currents have the same components as the photocycle [6, 7].

Subsequently dried oriented pm samples have been produced [8] which enable us to perform other meaningful experiments. In this paper, we report the results of studies on the very fast components of the electric signal in both oriented suspension and dried samples. In the latter case an external electric field was also applied to mimic the in vivo situation: the proteins in the cell work in the very high electric field of the membrane potential ($\sim 10^5$ V/cm). The effect of membrane potential on the lifetimes of the bR photocycle in bacteria has already been characterized by Dancsházy et al [9].

2. Materials and methods

The pm-s used in the measurements were separated by the usual procedure from Halobacterium halobium strain NRL R_1M_1 [10]. The apparatus utilized to measure the signals in solution was the same as in [5] with one important exception. The Keithley 604 differential amplifier was changed to a home made much faster differential amplifier. Fig. 2 shows response of this unit to a 1 μs square pulse switched in series with the pm solution. It can be seen that the time resolution of the amplifier is 0.2—0.3 μs if the signal is taken from a 10 kΩ resistance.

The preparation of dried, oriented samples was described in [8]. Minor modifications of the technique were necessary to enable us to conduct fast timings: the transparent, conducting SnO_2 layer had a resistance of $\sim 50\,\Omega$, and an Al layer was evaporated onto the dried pm layers. An external voltage of ~ 140 V was applied to the SnO_2 and Al electrodes when needed. Because ~ 2000 pm layers were in the sample,

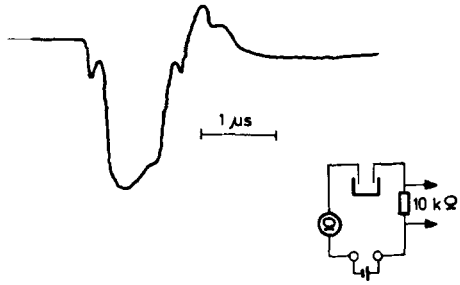

Fig. 2. Amplifier response to 1 μs square voltage switched in series with the pm solution (insert). Time resolution 0.1 μs

~70 mV potential was on a pm. The electric signals were registered at a resistance of ~1 kΩ switched parallel to the layer. Opton dye laser was used for excitation at a wavelength of 590 nm, a duration of 1 μs, and and energy ~10 mJ.

3. Results

a. pm-s oriented in suspension

The improved resolution of the electric circuit has made it possible to resolve the first negative component of the protein electric response signal (PERS) reported in [6] into the two components seen if Figs 3a, b. The temperature of the solution was maintained at 5 °C to obtain a clear discrimination between the first fast negative component and a second negative component having the lifetime of the $K \rightarrow L$ transition. The latter has been checked by observing the K-decay in light absorption measurement. Fig. 4 shows the fast component in an extended time scale. The signal increases during the 1 μs laser pulse and falls with the time constant of the electronics (~0.2—0.3 μs) after the light pulse is terminated.

The positive component in Figs. 3a, b corresponds to the $L \rightarrow M$ transition in accord with the previous assignment [6].

b. pm-s in dried oriented samples

The fast components of the PERS for dried oriented sample are very similar to the components in suspension. Fig. 5 shows the signal when no external field is applied to the sample. A large negative signal and a small positive signal appear, the latter containing two components. The time constants of these components differ from the corresponding time constants of bR-s in suspension. The same time constants appear in light absorption measurements, too.

In Fig. 5b a negative signal with very small amplitude and long lifetime is seen. Its area is nearly equal to the area of the positive signal in Fig. 5a. The signal does not have

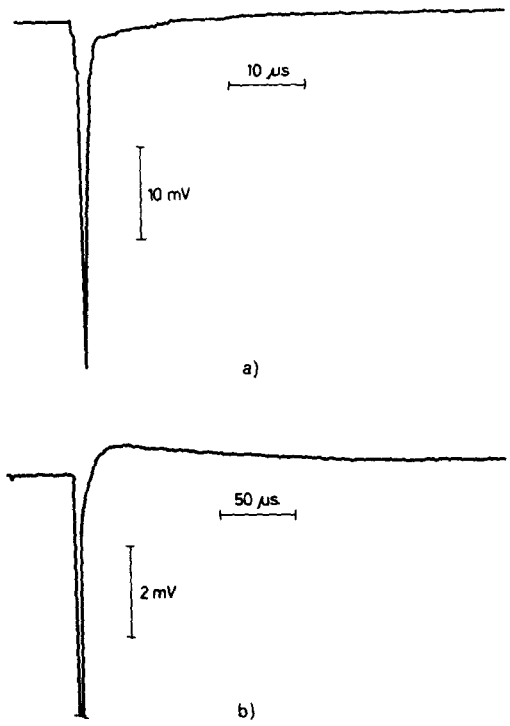

Fig. 3. The fast components of the PERS with different amplifications a, b. Orienting field $E = 15$ V/cm, absorbance of the pm suspension $A = 0.8$, temperature $T = 5$ °C. Recording from one flash

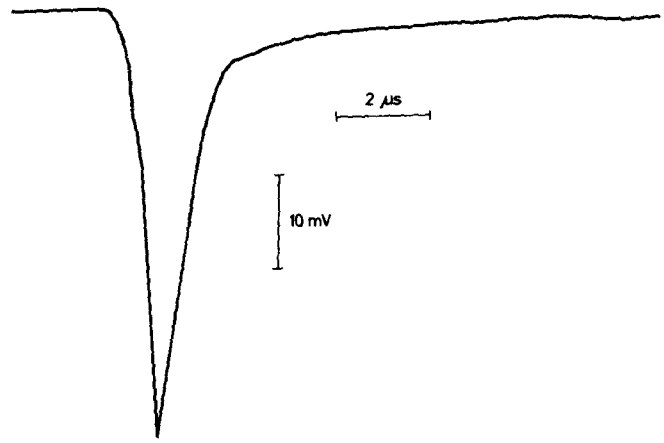

Fig. 4. The fast components of the PERS with extended time scale. The same record as in Fig. 3

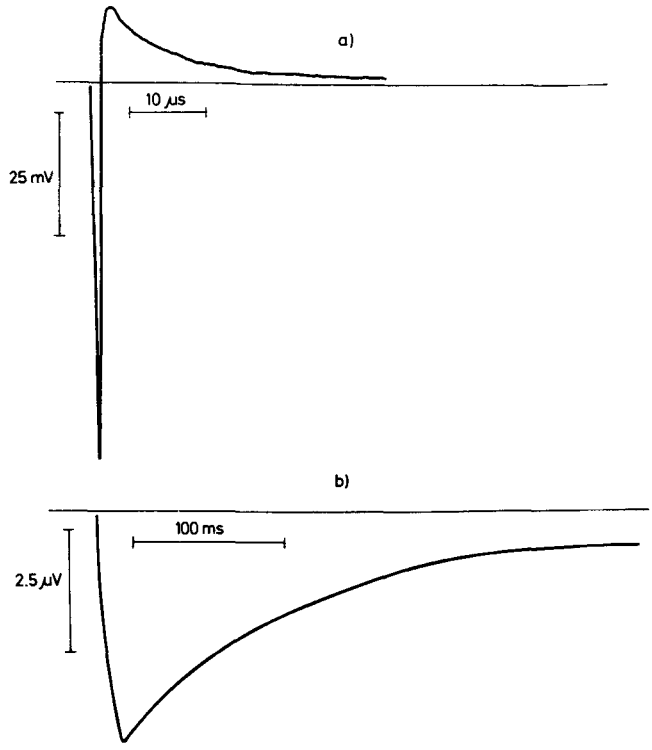

Fig. 5. The fast a) and slow b) components of the PERS in dried oriented sample. Signal taken from 1 kΩ resistance switched parallel to the sample

an analogue in the photocycle. This PERS can be understood as a backflow of protons from *M* state.

More details of the fast component can be observed in Figs 6a, b. In this series of measurements, data were produced in an externally applied electric field in the positive direction (+) (i.e. in the appropriate in vivo direction of proton flow) and in opposite direction (−). For comparison, we also measured the zero field situation. The electric field influences the PERS components: the first negative component has a larger amplitude in positive (+) and a smaller one in negative applied field (−) than the zero field signal (0). The peak positions and the decay times were also different. The decay time differences appear also in the positive components: they are longer in a (+) field and shorter in a (−) field than in the field free case. The data are summarized in Table I.

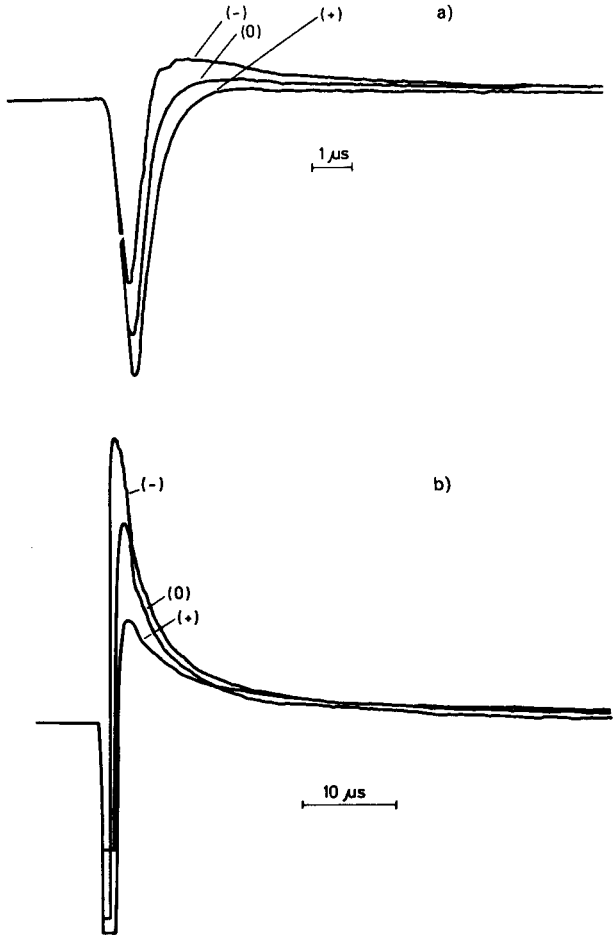

Fig. 6. The fast components of the PERS in external electric field. a, b, different amplifications and time scales. The voltage on ~2000 dried oriented layers was ±140 V. Signals taken from 1 kΩ resistance. (+), (−) and (0) signs refer to the field directions (see text) and to zero field

Table I

Amplitudes and time constants of the fast PERS components depending on electric field ((+), (−), (0) means field directions against and parallel to proton movement and zero field). A_1 amplitude, τ_1 decay time of the negative component, A'_3, A''_3, τ'_3, τ''_3 the same for the positive components. A-s in relative units, τ-s in μs. Area of the positive PERS components is $A'_3\tau'_3 + A''_3\tau''_3$ in relative units.

Field	A_1	τ_1	A'_3	τ'_3	A''_3	τ''_3	Area
+	90	0.62	2.2	5	1.35	39	64
0	78	0.54	4.5	4	1.3	31	60
−	62	0.45	6	3.1	1.9	26	68

4. Discussion

a. The protein electric response signal (PERS)

The PERS components were previously established [6] as the current which is induced in the external circuit by protons moving during the bR photocycle. More specifically, it is assumed that the proton at the protonated Schiff base of the lysine and retinal bond jumps to the external medium in two steps ($L \rightarrow M$, $M \rightarrow 0$ transitions) and that the missing proton from the Schiff base is then replaced from the internal side ($0 \rightarrow$bR transition). The negative PERS component has been assigned the to $K \rightarrow L$ transition as a reversed jump of the proton. This component has now been resolved into two components offering the possibility of a finer understanding of the first steps in the proton pumping mechanism of bR. For this reason a short recapitulation and extension of the theoretical basis for PERS originally given in [6] is needed. (A rather detailed theory of PERS is in preparation [11]).

The proton movement in bR causes induced current in the external circuit. If a charge Q moves with a velocity v between electrodes over a distance D then

$$i = \frac{Q}{D} v \tag{1}$$

is the value of the displacement current.

We assume that the velocity v is very large (since v has really no meaning for protons jumping from one position to another) and calculate the induced charge by integrating Eq. (1) for time:

$$Q_{\text{ind}} = \frac{Q}{D} \int_0^\infty v \, dt = \frac{Qd}{D}, \tag{2}$$

where d is the displacement of the charge. The measuring circuit is an RC circuit, and if a single Q_{ind} arrives, then a time course of voltage

$$V(t)_{(1)} = \frac{Qd}{D} \cdot \frac{1}{C} e^{-\frac{t}{RC}} \tag{3}$$

could be measured. In a laser flash many bR-s are excited, therefore many protons move (N). The number of moving protons per time unit ($\rho(N)$) in the case of an exponential decay is

$$\rho(N) = Nke^{-kt}, \tag{4}$$

where k is the rate constant. To get the wave form for N particles, Eqs. (3) and (4) must be folded:

$$V(t)_N = \frac{NQdk}{DC} \int_0^t e^{-kt'} e^{-\frac{t-t'}{RC}} \, dt' = \frac{NQdk}{D} \cdot \frac{R}{1-kRC} \left[e^{-kt} - e^{-\frac{t}{RC}}\right]. \tag{5}$$

Two limiting cases are important:

$$V(t)_N = \frac{NQdkR}{D} \cdot e^{-kt}, \quad \text{if} \quad k \ll \frac{1}{RC}, \tag{6a}$$

$$V(t)_N = \frac{NQd}{D}\frac{1}{C} e^{-\frac{t}{RC}}, \quad \text{if} \quad k \gg \frac{1}{RC}. \tag{6b}$$

In the above derivation it was tacitly assumed that the pm-s are in a medium of high resistance. This is the case in dried, oriented samples where the external R and C determine the circuit time constant. An $RC \sim 10^{-7}$ s can be estimated. In the case of the suspension R is the resistance and C is the capacitance of the electrolyte between the two sides of a pm. It can be estimated that $RC \sim 10^{-9}$ s. A realistic treatment must consider the data for pm-s, the R and C values of the solution and the measuring resistance [11]. For the present case, it is enough that the realistic treatment has the same time dependence as given in Eqs. (6a, b) and only the R and C values are somewhat modified. It is a good approximation that the RC of the external circuit (RC of the electronics, being $\simeq 0.2$—0.3 μs) is determining the measurements in suspension.

The lifetime of the bR→K transition is 16 ps (Fig. 1). The first negative PERS component should correspond to this transition because the second negative component in Fig. 3 has a lifetime of about 7 μs which corresponds to the $K \rightarrow L$ transition at 5 °C. Naturally we do not know without appropriate measurements that this charge movement also happens within 16 ps. Nevertheless, we may accept that this movement is much faster than the time constant RC, therefore, for the very fast component Eq. (6b), and for the following ones, Eq. (6a) may be applied.

The length of the laser flash is ~ 1 μs in our case and this is reflected in the ~ 1 μs continuous growth of the fast negative signal in Fig. 4. The folding of the moving charge per time unit for bR→K transition $\rho(n_K)$ and Eq. (3) is needed.

We assume, according to [12], that an S state appears after the photon-absorption which decays by the rate constant k_S to the K state.

Therefore

$$\begin{aligned} \dot{n}_{bR} &= -\sigma\phi n_{bR}, \\ \dot{n}_S &= +\sigma\phi n_{bR} - k_S n_S, \\ \dot{n}_K &= k_S n_S. \end{aligned} \tag{7}$$

Here n_{bR}, n_S, n_K are the normalized numbers of states, σ is the cross section to produce the state S, ϕ is the photon flux. Solving Eq. (7)

$$\dot{n}_K = \rho(n_K) = \frac{k_S \sigma\phi}{\sigma\phi - k_S}(e^{-k_S t} - e^{-\sigma\phi t}). \tag{8}$$

rom the folding

$$V_N(t) = \frac{NQd}{DC}\frac{k_S}{\sigma\phi - k_S}\left\{\frac{RC}{1-k_S RC}(e^{-k_S t} - e^{-\frac{t}{RC}}) - \frac{RC}{1-\sigma\phi RC}(e^{-\sigma\phi t} - e^{-\frac{t}{RC}})\right\}. \tag{9}$$

f $k_S \gg \frac{1}{RC}$ and $\sigma\phi \sim \frac{1}{RC}$, then

$$V_N(t) = \frac{NQd}{D}\frac{\sigma\phi R}{1-\sigma\phi RC}(e^{-\sigma\phi t} - e^{-\frac{t}{RC}}). \tag{10}$$

Eq. (10) is valid for 1 μs, after which the signal falls by the time constant RC. $V_N(t)$ has a flat maximum at $\sim 2\tau_{min}$, where τ_{min} is the smallest of time constants $\frac{1}{\sigma\phi}$ and RC. For $RC \simeq 0.2-0.3$ μs, and $\sigma\phi \simeq 1$, Eq. (10) describes Fig. 4 satisfactorily.

Eq. (10) and Fig. 4 could also be used to estimate d, the displacement of the charge in the bR→K transition. It is assumed that a single charge moves and excites the negative signal. The PERS of the $L \rightarrow M$ transition was also measured (Fig. 3) and the displacement for this transition is known to be $d_{L\rightarrow M} = 0.5$ nm from [6]. Using this value as a normalization for $\frac{NQ \cdot R}{D}$ (in the calculations Eq. (10) was applied with $RC = 0.3$ μs, $\sigma\phi = 1$ μs) $d_{bR\rightarrow K} \simeq 0.16$ nm. It is emphasized that this value is an estimated value only.

The assignment of the positive components of PERS in the dried, oriented samples is simple: they correspond to the $L \rightarrow M$ transition. The existence of two lifetimes (Table I) seems to reflect a branching of K decay to two different L states. Both τ_3', and τ_3'' are smaller in dried samples than the τ of the $L \rightarrow M$ transition in suspension. The external field accelerates (−) and decelerates (+) the transition.

Eq. (6a) can be used for the evaluation of the signal because $k_3' = \frac{1}{\tau_3'}$ and $k_3'' = \frac{1}{\tau_3''}$ are smaller than $\frac{1}{RC}$. The amplitude is proportional to the rate constant but the area of the signal must be constant if the number of excited bR-s N and the displacements d do not change. Table I contains the area of the positive signals for the different external fields as calculated from amplitudes and time constants.

The results show that the external fields change only the transition times and not the area proportional to Nd. We assume that d is given by the structure of the molecule which is not influenced by the electric field therefore the number of excited states N or with other words the cross section for bR→K transition σ is not influenced by the external fields (the constancy is within ±8%). This would mean a constant amplitude of the negative signal according to Eq. (10) because even RC of the circuitry is

Table II
Distances determined from PERS
(data in nm)

Transition	d [nm]
1. br→K	−0.16
2. K→L	−0.05
3. L→M	+0.5
4. M→0	3.0
5. 0→bR	1.5

independent of the external field. The values of A_1 in Table I, however, contradict the above requirements.

A closer examination of the curves in Fig. 6a and Fig. 4, however, resolves the problem. It is clear that the transition from negative to positive peak needs time. This is the time constant of the $K \rightarrow L$ transition. In Fig. 3 and $4\tau_{K\rightarrow L} = 7$ μs is much longer than the 1 μs laser flash, therefore it does not disturb the negative peak. In dry samples the time constants are much shorter, $\tau_{K\rightarrow L}$ is $\simeq 0.5$ μs, which can be seen in Table I. The recharging already occurs during the flash therefore Eq. (10) should be modified by adding an exponential with opposite sign. The electric field influences $\tau_{K\rightarrow L}$ also in qualitatively the same way as τ_3' and τ_3'' (Table I). The amplitude of an exponential is proportional to $k = \frac{1}{\tau}$ (Eq. 6a) therefore a larger amplitude should be subtracted for field (−) than for field (+). The data A_1 and τ_1 in Table I agree qualitatively with this explanation. τ_1 in Table I is the resultant of $\tau_{K\rightarrow L}$, RC and $\sigma\phi$. To determine $\tau_{K\rightarrow L}$ requires a better time resolution by the electronics and a shorter laser pulse. For the present, we may state that the electric field changes the time constants of the transitions $K \rightarrow L$, $L \rightarrow M$ in a similar way and does not change the cross section σ. The time constant of bR→K may also be changed, but this is beyond the limit of our time resolution.

b. A model of bR proton pump

The data extracted from the measurement of PERS [6, 7 and present work] indicate charge movement which occurs in 5 steps in the protein. The distances were determined by assuming that the PERS-s are the consequences of proton movement and not the movement of some charged amino acid side chains. In Table II we recapitulate the data for these distances including the presently determined distance for the bR→K transition.

One can see that the distances represent two distinct groups: (1) small ones (<0.5 nm, transitions 1., 2., and 3.,) and (2) large ones (4., 5.,). It is generally accepted that the protons originate from the protonated Schiff base which is at a distance of

1.4—1.5 nm from the internal surface of the membrane. Therefore the movements in group (1) must occur deep in the protein. We call these movements internal movements. In transitions 4. and 5., the protons are released to and enter from the environments, they may be called external movements. In dried samples, the internal time constants become shorter and the external constants longer. These facts support our grouping of the transitions.

We can speculate about the nature of the proton donating and accepting sites. To do this we must consider other data in addition to the optical data of the photocycle in visible and PERS-data:

— Laser Raman spectroscopy indicates that the Schiff base is deprotonated during $L \rightarrow M$ decay, and it is reprotonated when bR ground state is reestablished [1].

— UV absorption changes show that both a tyrosine and a tryptophan side chain participate in the proton translocation function of bR [13, 14, 15]. More specifically, a tryptophan is disturbed by a proton approaching it [15]. The rise time of this event coincides with the $K \rightarrow L$ transition [14], the decay time with the $M \rightarrow 0$ transition or the $M(\rightarrow 0) \rightarrow$bR transition, but we cannot decide which from the existing data [14, 15]. We assume it happens after the M decay. A tyrosine becomes deprotonated with rise time of the $L \rightarrow M$ transition [14] and reprotonated with the same timing as the tryptophan.

The events in the five transitions may be described by the following model (Fig. 7):

(1) In the bR ground state the retinal is bound by the protonated Schiff base lysine 216 (or 41). The N^+ is compensated for by the negative charge of a close residue (A_1^-) which could belong to an aspartic or glutamic acid. The distance between H^+ and A_1^- is ~ 0.2 nm. Near the Schiff base is a TRP and also a TYR residue. For the following discussion we assume the existence of another residue, A_2^-, which is protonated in bR ground state A_2H. The situation is depicted in Fig. 7 (1).

The ground state retinal is in an all-trans configuration, and this is transformed into the 13-cis configuration by photon absorption. The trans-cis isomerization involves an inward movement (Fig. 7 (1) (2)) of the H^+N group with the salt bridge between H^+N and A_1^- being broken and the new position is stabilized [16, 17]. This means that the energy barrier for cis-trans transition is high. From the geometry it can be calculated that the inward displacement of the H^+ $d_{1\text{geom}||}$ is 0.16 nm, and the lateral one is $d_{1\text{geom}\perp}$ 0.2 nm. The fast negative portion of the PERS corresponds to the inward motion of the proton. The estimated value of charge displacement $d_1 \sim 0.16$ nm is in good agreement with $d_{1\text{geom}||}$. A large lateral movement is expected in accord with Fig. 7 (1). We have H^+N and A_1^- in a distance of $\simeq 0.5$ nm. The energy transformed into electrical energy and stored is $\simeq 0.2$ aJ ($\sim 60\%$ of the energy of absorbed photon).

(2) In the $K \rightarrow L$ transition the proton from A_2H moves a small distance d_2 inward and disturbs the TRP residue (Fig. 7 (2)). After this transition, in the L state there are four uncompensated charges in the molecule, A_1^-, A_2^-, $TRPH^+$ and H^+N.

(3) We have to assume that the $L \rightarrow M$ transition has two proton movements: both the Schiff base and a TYR are deprotonated simultaneously. We postulate that

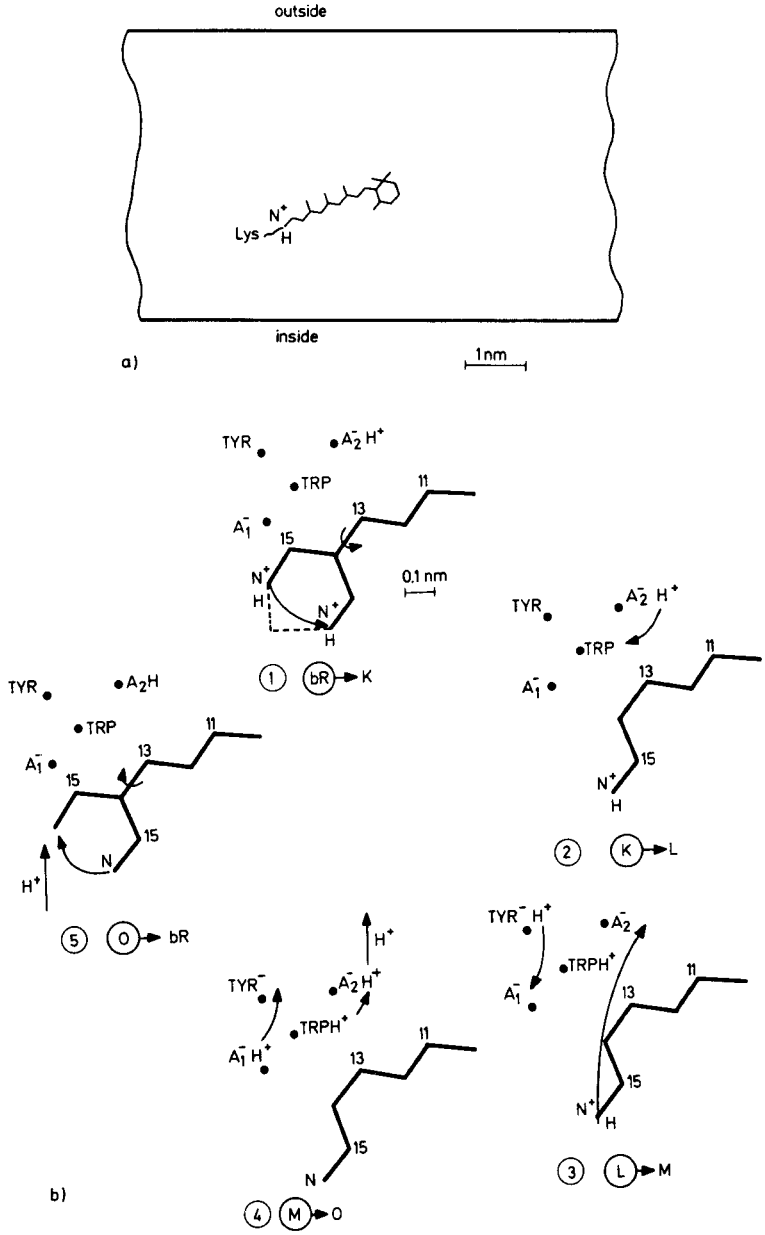

Fig. 7. Geometrical model of the bacteriorhodopsin proton pump. a. The location of the retinal in the bR molecule. b. The magnified (5 times) neighbourhood of the Schiff base (1), (2), (3), (4) and (5) represent the bR ground state, *K*, *L*, *M* and *O*-states. Arrows show the assumed transitions from the given states

the Schiff base proton moves to the A_2^- while the TYR proton moves to the A_1^- forming A_2H, A_1H and TYR^-. The algebraic sum of the two distances $d_3 = d_{3\text{Schiff}} + d_{3\text{TYR}} = 0.5$ nm. We think that the $d_{3(\text{Schiff})}$ is the dominant shift and it is directed outward (i.e. it is positive) and that $d_{3(\text{TYR})}$ is smaller and negative. The *M* state is characterized then by a $TRPH^+$ and a TYR^-. Note that the original dipole NH^+ and A_1^- in *K* state (1) is shifted outwards.

(4) The *M* decay is the most important step during proton pumping and also the most complicated in the present model. Three proton movements must happen during this rearrangement.

The dipole field of $TRPH^+$ and TYR^- expels the proton from the A_2H barrier to the external surface. This displacement is $d_4 \sim 3$ nm. The assumed small proton movements of $TRPH^+ \rightarrow TRP + A_2H$ and $A_1H \rightarrow TYR + A_1^-$ are negligible in comparison with d_4.

The small internal proton movements can probably be accounted for as jumps between neighbouring positions. The 3 nm external movement, however, requires further clarification. The long lifetime of the *M* state $\tau_M \simeq 10$ ms indicates the low probability with which the proton will leave the A_2^- barrier. Once the proton has overcome the $A_2H - A_2^-$ barrier its pathway is a straightforward move to the surface using the so-called proton wire which has been substantiated as a network of hydrogen bonded side chains [18, 19, 20, 21]. The proton current is conducted similar to the current which occurs in ice. An upper time limit estimate for this conduction is ~ 1 μs, which is negligible when compared with τ_M.

We now suggest another mechanism for proton conductance which does not require the specific structure of hydrogen bounded chains. It is well known that fluctuations in protein structure can make any part of a protein accessible to water molecules [22, 23]. This is a rather fast process (in some cases it is in the ms range) as indicated from measurement of H – D exchange of peptide hydrogens in proteins [24]. The H can be exchanged only when a D_2O molecule is in very close proximity.

We assume that the A_2H can only be deprotonated when an H_2O appears and binds the proton forming a hydroxonium ion (H_3^+O), which is then expelled by the electrostatic forces of the existing dipole. τ_M then reflects both the time necessary for an H_2O to appear and the height of the barrier for protons to leave A_2^-. After proton exchange the time for the H_3^+O to move to the surface is short [25]. This type of proton conducting mechanism can explain the tremendous increase (100—1000 times) of the *M* lifetime in the dried samples and the missing proton extrusion (Fig. 5). This explanation is in line with the current concept of protein fluctuations [26].

In the *O* state, one proton is outside at the external surface of the bR molecule and one charged group A_1^- remains inside.

(5) The $O \rightarrow$ bR transition is characterized by a cis-trans isomerization of the retinal. The N group moves back to its original position and is protonated from inside the membrane. This protonation is also by external interaction and occurs by the same mechanism outlined in (4). The height of the barrier to this step is determined by the

barrier of the cis-trans isomerization and the availability of a proton conducted as H_3^+O.

The model outlined above explains all the known facts of the bR photocycle available from visual, UV, Laser Raman spectroscopy and the measured PERS-s. The effects of the electric fields on the lifetimes measured by Dancsházy et al [9] and in this work (Figs 5, 6) are easily understood: the barriers for proton jumps are increased (+) or decreased (−).

The back photeraction, i.e. the termination of proton pumping and the reappearance of bR ground state from M state under the effect of blue light which is connected with spectral [27] and PERS changes [7] is accommodated by the model: In M state, the retinal absorbs a photon and undergoes a rapid cis-trans isomerization. Note that the Schiff base is neutral in M state. This induces the release of a proton from $A_1^-H^+$ to TYR^- causing a small fast positive electric signal. This has actually been observed in [7]. The next step is the reprotonation of the Schiff base from A_2H leaving A_2^- to be reprotonated from $TRPH^+$. If these steps are separated two additional components can exist in visual light spectroscopy as observed in [14].

The retinal in *M* state may have a spontaneous cis-trans transition with a very long lifetime of ~ 100 ms. If the *M* state is unable to decay in the dry sample because of the absence of H_2O then the back reaction which is initiated by spontaneous cis-trans transition shortcuts the proton pump. This explains the slow negative signal observed in Fig. 5b.

An inherent difficulty in this model is the assumption of multiple events in some of the transitions (2 in (3), 3 in (4) and 2 in (5)). This could, however, actually be advantageous in explaining the existence of two time constants measured for the *L*-decay here, and also reported by many authors, e.g. [14]. These brachings are reported to exist under unusual circumstances such as dryness, low temperature, non physiological pH, modified bR, ...).

There are a growing number of papers which indicate that two protons are probably pumped per photocycle (for a review see [29]). Our model has enough flexibility to accommodate this requirement by making small modifications: one proton may transfer via the Schiff base and A_2^-, while the other proton is transported via the TYR^- side chain and A_1^-.

This model is largely dependent on structural informations. It requires the existence of a TYR, TRP and two carboxyl groups (A_1^-, A_2^- from aspartic our glutamic acid) at the appropriate distances from the Schiff base.

One should find the characteristic absorption changes for $A_1^- + H^+$, $A_2^- + H^+$ with the forecasted time constants in the short wavelength UV region. The lateral motions of these charges could confirm the structural assignments. The easiest distance to measure seems to be $d_{1\,\mathrm{geom}\perp}$ which must exist in a given relationship to $d_{1\,\mathrm{geom}||}$ which has already been measured.

The time of appearance of the pumped proton in the solution is crucial. It should happen in the *M* decay.

Variations in photocycle due to specific modifications of bR side chains could also help in critical checks of the model.

We may consider the velocity of proton movements in the external transitions ($M \rightarrow O$, $O \rightarrow$ bR) as a possibility to decide between the different proton wire models (i.e. hydrogen bonded chains or H_2O channel produced by protein fluctuation). In Eq. (2) the velocity was assumed to be very large for all transitions. Final velocity, however, can be included in Eq. (3) and finally in Eq. (5) [11] offering a means for experimental control.

Discussions related to the proposed model with Prof. W. Stoeckenius are highly acknowledged.

References

1. W. Stoeckenius, R. H. Lozier and R. A. Bogomolni, Biochim. Biophys. Acta, **505,** 215, 1979.
2. P. Mitchell, Nature, **191,** 144, 1961.
3. L. A. Drachev, A. D. Kaulen and V. P. Skulachev, FEBS Lett., **87,** 161, 1978.
4. F. T. Hong and M. Montal, Biophys. J., **25,** 465, 1979.
5. L. Keszthelyi, Biochim. Biophys. Acta, **598,** 429, 1980.
6. L. Keszthelyi and P. Ormos, FEBS Lett., **109,** 189, 1980.
7. P. Ormos, Zs. Dancsházy and L. Keszthelyi, Biophys. J., **31,** 207, 1980.
8. Gy. Váró, Acta Biologica Hung., **32,** 301, 1981.
9. Zs. Dancsházy, S. Helgerson and W. Stoeckenius, to be published.
10. D. Oesterhelt and W. Stoeckenius, Methods in Enzymology, **31,** 667, 1974.
11. P. Ormos and L. Keszthelyi, to be published.
12. M. L. Applebury, K. Peters and P. Rentzepis, Biophys. J., **23,** 375, 1978.
13. R. A. Bogomolni, in Bioelectrochemistry ed. by H. Keyzer and F. Guttman, Plenum Publishing Corp. p. 83., 1980.
14. B. Hess and P. Kuschmitz, FEBS Lett., **100,** 334, 1979.
15. J. Czégé, A. Dér, L. Zimányi and L. Keszthelyi, Proc. Natl. Acad. Sci. **79,** 7273, 1982.
16. B. Honig, T. Ebrey, R. H. Callender, U. Dinur and M. Ottolenghi, PNAS, **76,** 2503, 1979.
17. A. Warshel, Photochem. Photobiol. **30,** 285, 1979.
18. J. F. Nagle, M. Mille and H. J. Morowitz, J. Chem. Phys., **72,** 3959, 1979.
19. J. F. Nagle and M. Mille, J. Chem. Phys., **74,** 1367, 1981.
20. W. Stoeckenius in Membrane Transduction Mechanisms, ed. by R. A. Cone and J. E. Dowling, Raven, New York, p. 39, 1979.
21. H. Merz and G. Zundel, Biochem. Biophys. Res. Comm., **101,** 540, 1981.
22. F. M. Richards, Ann. Rev. Biophys. Bioenerg., **6,** 151, 1977.
23. F. M. Richards, Abstracts of the VII. International Biophys. Congress, Mexico City, p. 14, 1981.
24. J. Rose, J. Mol. Biol., **113,** 143, 1979.
25. P. Läuger, Biochim, Biophys. Acta, **552,** 143, 1979.
26. H. Frauenfelder, G. A. Petsko and D. Tsernoglou, Nature, **280,** 558, 1979.
27. O. Kalinsky, U. Lachish and M. Ottolenghi, Photochem. Photobiol., **28,** 261, 1978.
28. F. F. Litvin and S. P. Balashov, Biofizika, **22,** 1111, 1977.
29. R. A. Bogomolni, R. A. Baker, R. H. Lozier and W. Stoeckenius, Biochemistry, **19,** 2152, 1980.